

Unexpected Aliovalent Cation Substitution Between Two NLO Materials

LiBa₃Bi₆(SeO₃)₇F₁₁ and Ba₃Bi_{6.5}(SeO₃)₇F_{10.5}O_{0.5}

Shuangshuang Shi,^{ab} Chensheng Lin,^d Dan Zhao,^e Min Luo,^{*a} Liling Cao,^{ab} Guang Peng^a and Ning Ye ^{*ac}

^a Key Laboratory of Optoelectronic Materials Chemistry and Physics, Fujian Institute of Research on the Structure of Matter, Chinese Academy of Sciences, Fuzhou, Fujian 350002, China.

^b University of the Chinese Academy of Sciences, Beijing 100049, China.

^c Fujian Science & Technology Innovation Laboratory for Optoelectronic Information of China, Fuzhou, Fujian 350002, China.

^d State Key Laboratory of Structural Chemistry, Fujian Institute of Research on the Structure of Matter, Chinese Academy of Science, Fuzhou, Fujian 350002, China.

^e Department of Physics and Chemistry, Henan Polytechnic University, Jiaozuo, Henan 454000, China.

E-mail: nye@fjirsm.ac.cn

E-mail: lm8901@fjirsm.ac.cn

Table of Contents

Experimental section	LBBsf and BBSF	S3
Table S1	The experimental data of birefringence measurements for LBBsf and BBSF	S5
Table S2	Crystal Data and Structure Refinement for LBBsf and BBSF	S6
Table S3	Atomic coordinates ($\times 10^4$), equivalent isotropic displacement parameters ($\text{\AA}^2 \times 10^3$) for LBBsf	S7
Table S4	Selected bond lengths [\AA] and angles [deg] for LBBsf	S7
Table S5	Anisotropic displacement parameters ($\text{\AA}^2 \times 10^3$) for LBBsf	S9
Table S6	Atomic coordinates ($\times 10^4$), equivalent isotropic displacement parameters ($\text{\AA}^2 \times 10^3$) for BBSF	S9
Table S7	Selected bond lengths [\AA] and angles [deg] for BBSF	S10
Table S8	Anisotropic displacement parameters ($\text{\AA}^2 \times 10^3$) for BBSF	S11
Table S9	The calculated dipole moments of the Bi-O(F) polyhedra and SeO_3 units	S12
Figure S1	Experimental and calculated powder XRD for LBBsf and BBSF	S13
Figure S2	TG and DTA curves of LBBsf and BBSF	S13
Figure S3	The coordination of Bi atoms of multimers and the alignment of $[\text{SeO}_3]$ groups in LBBsf and BBSF	S14
Figure S4	UV-Vis-NIR diffuse reflectance spectra of LBBsf and BBSF	S15
Figure S5	IR transmittance spectra of LBBsf and BBSF	S16
Figure S6	The calculated band structures of LBBsf and BBSF	S17
Figure S7	The scissor-added partial density of states (PDOS) for LBBsf and BBSF	S17
Figure S8	Calculated frequency-dependent SHG coefficients of LBBsf and BBSF	S18
Figure S9	Calculated refractive indices and birefringence of LBBsf and BBSF	S18
Figure S10	Photographs of LBBsf and BBSF for measurements of birefringence.	S19
Reference		S19

Experimental section

Reagents

Bi_2O_3 (99.0%), SeO_2 (99.0%), LiF (99.0%) (Shanghai Macklin Biochemical Co., Ltd.), BaF_2 (99.0%), BaO (97.0%) (Sinopharm Chemical Reagent Co., Ltd.) and 40.0% solution of HF (Tansoole Chemical Reagent Co., Ltd.) were obtained commercially and used as received.

Synthesis

Single crystals of **LBSF** and **BBSF** were grown through a facile hydrothermal method under subcritical conditions.

Synthesis of LBSF. A mixture of BaF_2 (702 mg, 4.0 mmol), Bi_2O_3 (932 mg, 2 mmol), SeO_2 (888 mg, 8.0 mmol), LiF (156 mg, 6.0 mmol), 40.0% solution of HF (0.4 mL) and 7 mL H_2O was sealed in an autoclave with a 23 mL-Teflon liner and heated at 270 °C for four days, followed by slowly cooling to 30 °C at 3 °C/h. After being washed with deionized and ethanol and then dried in air, colorless prism-shaped crystals were obtained in 55% yield based on Bi.

Synthesis of BBSF. A mixture of BaO (614 mg, 4.0 mmol), Bi_2O_3 (932 mg, 2 mmol), SeO_2 (888 mg, 8.0 mmol), 40.0% solution of HF (0.3 mL) and 10 mL H_2O was sealed in the same autoclave as above. The other following steps were the same as described above, giving colorless prism-shaped crystals with 50% yield based on Bi.

Single-crystal X-ray diffraction

Colorless transparent prism-shaped crystals of **LBSF** and **BBSF** were chosen to mount on a thin glass fiber with epoxy for single-crystal XRD data collection, which were collected at room temperature on a Rigaku Mercury CCD diffractometer with graphite-monochromatic $\text{Mo K}\alpha$ radiation ($\lambda = 0.71073 \text{ \AA}$). The data were integrated with the program CrystalClear. The intensities were corrected for Lorentz polarization, air absorption, and absorption attributable to the variation in the path length through the detector faceplate. Absorption corrections were also applied relied on the Multi-scan technique. Their structures were established by the direct method and refined on F^2 by using difference Fourier maps and full-matrix least-squares techniques with SHELXL-97.¹ The structures were verified by the ADDSYM algorithm from the PLATON

program,² and no other higher symmetries were found. The detailed crystallographic data and structural refinement parameters of **LBSF** and **BBSF** were summarized in **Table 1**. Selected bond lengths, atomic coordinates, equivalent isotropic displacement parameters, and anisotropic displacement parameters were listed in **Tables S2–S7** of the Supporting Information.

Powder X-ray diffraction

Powder XRD (PXRD) patterns of polycrystalline materials were recorded on a Miniflex600 powder X-ray diffractometer using Cu K α radiation ($\lambda = 1.540598 \text{ \AA}$), with a scan step size of 0.02°, scan time of 0.2s in the angular range (2θ) of 5 – 75°. The experimental PXRD patterns for both compounds were very consistent with the corresponding calculated data from the single-crystal models.

Thermal analysis

The TG analyses were measured on a NETZSCH STA449F3 thermal analyzer instrument. Reference (Al_2O_3 crucible) and crystal samples loaded in the same crucible were heated from 30 to 1000 °C at a rate of 10 °C/min under flowing nitrogen gas.

UV-vis-NIR diffuse reflectance spectroscopy

The UV-vis-NIR diffuse reflectance spectra of two compounds were conducted on a PerkinElmer Landa-950 UV-vis-NIR spectrophotometer in the range of 200-2500 nm with BaSO_4 as a standard. The reflectance spectra were converted to absorbance spectra with the Kubelka-Munk function^{3, 4}: $F(R) = (1 - R)^2/2R = K/S$, where R , S , and K represent the reflectance, scattering factor and absorption coefficient, respectively. The linear fitting extrapolation of $[F(R)hv]^2$ versus hv plot were carried out to calculate the direct band gap (and $[F(R)hv]^{1/2}$ versus hv plot for indirect band gap)⁵.

Infrared Spectroscopy

The infrared transmittance spectra of LBSF and BBSF were recorded by using a Bruker VERTEX 70 Fourier spectrometer covering the wavenumber range 4000-400 cm^{-1} . The powder samples diluted with dry KBr (mass ratio about 1:100) were pressed into transparent sheets for measurements.

Birefringence

The birefringence of LBSF and BBSF were tested on a polarizing microscope

(ZEISS Axio Scope. A1) equipped with a Beker compensator. The wavelength of light source was 546.1 nm. In order to improve the accuracy, clean and transparent lamellar crystals were selected. The formula of birefringence calculation was as follows:

$$\Delta R \text{ (retardation)} = \Delta n \times T$$

ΔR , Δn , T represent the optical path difference, birefringence and the thickness of the crystal, respectively. The measured birefringences were calculated to be 0.130 and 0.121 @546.1 nm for **LBSF** and **BBSF** (Table 2), respectively.⁶

Table S1. The experimental data of birefringence measurements for **LBSF** and **BBSF**.

Crystal	ΔR (nm)	T (μm)	Δn (exp.)
LBSF	1020	7.82	0.130
BBSF	1570	13.02	0.121

Second-harmonic generation

The SHG signals of polycrystalline samples were investigated by the Kurtz-Perry⁷ method. A Q-switched Nd:YAG solid-state laser was used for providing 1064 nm laser light source. Since SHG efficiencies significantly depend upon particle sizes, crystalline samples of **LBSF** and **BBSF** were ground and sieved into distinct particle-size ranges (25-45, 45-62, 62-75, 75-109, 109-150 and 150-212 μm). The samples were pressed between glass slides and secured with aluminum holders containing 8-mm diameter hole in the middle. Sieved KH_2PO_4 (KDP) samples in corresponding particle size ranges were used for making references.

First-principles calculations

Electronic band structure, density of states (DOS)/ partial DOS and optical properties for two compounds were investigated through the first-principles calculation with the density functional theory (DFT) in the CASTEP suite of program.⁸

⁹ The following orbital electrons of component elements were considered in the computation: Li 2s¹, Ba 5s²5p⁶6s², Bi 5d¹⁰6s²6p³, Se 4s²4p⁴, O 2s²2p⁴ and F 2s²2p⁵. Generally, the exchange and correlative potential of electron-electron interactions were described by Perdew-Burke-Eruzerhof (PBE) functional with generalized gradient approximation (GGA). The effective interactions between ionic cores and electrons

were represented through the norm-conserving pseudopotentials¹⁰ in the Kleinman-Bylander form. A Monkhorst-Pack¹¹ scheme k -pointing sampling size of 2x2x2 and 1x1x1 were used in the first Brillouin zone of the unit cell. A plane wave energy cutoff was set to be 850 eV. The self-consistent convergence of the total energy was 1.0×10^{-5} eV/atom. Because of the underestimation of band gap by the DFT method, the scissor operation¹² was taken in the dielectric function calculation. The “velocity-gauge” formula¹³ was used for evaluating SHG coefficients and “band-resolved” method¹⁴ was employed to calculate SHG-weighted density.

Table S2. Crystal Data and Structure Refinement for **LBSF** and **BBSF**.

Formula	LiBa ₃ Bi ₆ (SeO ₃) ₇ F ₁₁	Ba ₃ Bi _{6.5} (SeO ₃) ₇ F _{10.5} O _{0.5}
<i>Fw</i>	2770.56	2866.55
Temperature (K)	293(2)	293(2)
Crystal System	Trigonal	Trigonal
Space Group	<i>P3₁m</i>	<i>P3₁m</i>
Crystal habit	Prism	Prism
Crystal color	Colorless	Colorless
<i>a</i> (Å)	9.340(3)	9.479(3)
<i>b</i> (Å)	9.340(3)	9.479(3)
<i>c</i> (Å)	9.710(5)	9.566(4)
α (deg)	90	90
β (deg)	90	90
γ (deg)	120	120
<i>V</i> (Å ³)	733.6(5)	744.4(5)
<i>Z</i>	1	1
<i>Dc</i> (Mg/m ³)	6.271	6.395
λ (Å)	0.71073	0.71073
<i>F</i> (000)	1174	1212
μ (mm ⁻¹)	48.632	50.867
<i>R/wR</i> ($I > 2\sigma(I)$) ^a	0.0256 / 0.0477	0.0312 / 0.0646
<i>R/wR</i> (all data) ^a	0.0269 / 0.0481	0.0326 / 0.0650
GOF on <i>F</i> ²	0.879	1.131
Absolute Structure Parameter	-0.003(9)	0.031(11)

^a $R(F) = \sum | |Fo| - |Fc| | / \sum |Fo|$. $wR(Fo^2) = [\sum w(Fo^2 - Fc^2)^2 / \sum w(Fo^2)^2]^{1/2}$

Table S3. Atomic coordinates ($\times 10^4$), equivalent isotropic displacement parameters ($\text{\AA}^2 \times 10^3$) forLiBa₃Bi₆(SeO₃)₇F₁₁.

	x	y	z	U(eq)
Bi(1)	-7583(1)	0	-3269(1)	10(1)
Bi(2)	-7386(1)	0	1004(1)	15(1)
Ba(1)	-10000	-3946(1)	-6071(1)	12(1)
Se(1)	-3897(2)	0	-1031(2)	9(1)
Se(2)	-6667	-3333	-3464(2)	10(1)
Se(3)	-6667	-3333	1581(2)	9(1)
O(1)	-8037(8)	-5114(8)	2445(7)	10(2)
F(1)	-10000	-2641(8)	-3619(9)	15(2)
F(2)	-8191(10)	0	-5373(8)	15(2)
O(2)	-8237(9)	-4965(9)	-4290(7)	14(2)
F(3)	-10000	0	41(17)	35(5)
O(3)	-1933(8)	1680(9)	-889(8)	17(2)
O(4)	-4768(11)	0	509(10)	17(3)
F(4)	-11694(9)	0	-7783(8)	14(2)
F(5)	-10000	0	-2637(17)	27(4)
Li(1)	-10000	0	-6510(30)	1(8)

U(eq) is defined as one third of the trace of the orthogonalized U_{ij} tensor.**Table S4.** Selected bond lengths [Å] and angles [deg] for LiBa₃Bi₆(SeO₃)₇F₁₁.

Bi(1)-F(2)	2.120(7)	O(3)#5-Bi(2)-O(1)#2	148.6(2)
Bi(1)-F(5)	2.339(4)	O(1)#1-Bi(2)-O(1)#2	81.4(3)
Bi(1)-O(2)#1	2.377(7)	O(3)#4-Bi(2)-F(4)#6	137.5(2)
Bi(1)-O(2)#2	2.377(7)	O(3)#5-Bi(2)-F(4)#6	90.7(3)
Bi(1)-F(1)	2.393(5)	O(1)#1-Bi(2)-F(4)#6	72.1(2)
Bi(1)-F(1)#3	2.393(5)	O(1)#2-Bi(2)-F(4)#6	115.0(2)
Bi(2)-O(3)#4	2.413(8)	O(3)#4-Bi(2)-F(4)#7	90.7(3)
Bi(2)-O(3)#5	2.413(8)	O(3)#5-Bi(2)-F(4)#7	137.5(2)
Bi(2)-O(1)#1	2.436(7)	O(1)#1-Bi(2)-F(4)#7	115.0(2)
Bi(2)-O(1)#2	2.436(7)	O(1)#2-Bi(2)-F(4)#7	72.1(2)
Bi(2)-F(4)#6	2.447(4)	F(4)#6-Bi(2)-F(4)#7	68.1(4)
Bi(2)-F(4)#7	2.447(4)	O(3)#4-Bi(2)-O(4)	80.8(3)
Bi(2)-O(4)	2.492(11)	O(3)#5-Bi(2)-O(4)	80.8(3)
Bi(2)-F(3)	2.614(6)	O(1)#1-Bi(2)-O(4)	68.0(2)

Se(1)-O(4)	1.702(10)	O(1)#2-Bi(2)-O(4)	68.0(2)
Se(1)-O(3)	1.722(7)	F(4)#6-Bi(2)-O(4)	139.0(2)
Se(1)-O(3)#16	1.722(7)	F(4)#7-Bi(2)-O(4)	139.0(2)
Se(2)-O(2)#2	1.698(7)	O(3)#4-Bi(2)-F(3)	74.9(3)
Se(2)-O(2)	1.698(7)	O(3)#5-Bi(2)-F(3)	74.9(3)
Se(2)-O(2)#17	1.698(7)	O(1)#1-Bi(2)-F(3)	131.9(2)
Se(3)-O(1)#2	1.727(7)	O(1)#2-Bi(2)-F(3)	131.9(2)
Se(3)-O(1)	1.727(7)	F(4)#6-Bi(2)-F(3)	62.8(3)
Se(3)-O(1)#17	1.727(7)	F(4)#7-Bi(2)-F(3)	62.8(3)
F(2)-Bi(1)-F(5)	89.7(5)	O(4)-Bi(2)-F(3)	147.9(4)
F(2)-Bi(1)-O(2)#1	77.4(3)	O(4)-Se(1)-O(3)	102.8(3)
F(5)-Bi(1)-O(2)#1	140.2(2)	O(4)-Se(1)-O(3)#16	102.8(3)
F(2)-Bi(1)-O(2)#2	77.4(3)	O(3)-Se(1)-O(3)#16	104.2(5)
F(5)-Bi(1)-O(2)#2	140.2(2)	O(2)#2-Se(2)-O(2)	99.5(3)
O(2)#1-Bi(1)-O(2)#2	73.7(4)	O(2)#2-Se(2)-O(2)#17	99.5(3)
F(2)-Bi(1)-F(1)	75.5(2)	O(2)-Se(2)-O(2)#17	99.5(3)
F(5)-Bi(1)-F(1)	67.93(19)	O(1)#2-Se(3)-O(1)	98.4(3)
O(2)#1-Bi(1)-F(1)	140.2(3)	O(1)#2-Se(3)-O(1)#17	98.4(3)
O(2)#2-Bi(1)-F(1)	72.4(2)	O(1)-Se(3)-O(1)#17	98.4(3)
F(2)-Bi(1)-F(1)#3	75.5(2)	Bi(1)-F(1)-Bi(1)#15	109.6(3)
F(5)-Bi(1)-F(1)#3	67.93(19)	Bi(2)#3-F(3)-Bi(2)	108.0(4)
O(2)#1-Bi(1)-F(1)#3	72.4(2)	Bi(2)#3-F(3)-Bi(2)#15	108.0(4)
O(2)#2-Bi(1)-F(1)#3	140.2(3)	Bi(2)-F(3)-Bi(2)#15	108.0(4)
F(1)-Bi(1)-F(1)#3	126.4(3)	Bi(2)#21-F(4)-Bi(2)#22	119.5(3)
O(3)#4-Bi(2)-O(3)#5	80.8(3)	Bi(1)#15-F(5)-Bi(1)#3	113.4(3)
O(3)#4-Bi(2)-O(1)#1	148.6(2)	Bi(1)#15-F(5)-Bi(1)	113.4(3)
O(3)#5-Bi(2)-O(1)#1	90.5(2)	Bi(1)#3-F(5)-Bi(1)	113.4(3)
O(3)#4-Bi(2)-O(1)#2	90.5(2)		

Symmetry transformations used to generate equivalent atoms:

```
#1 y,x+1,z  #2 -x+y-1,-x-1,z  #3 -y-1,x-y+1,z  #4 y-1,x,z  #5 -x+y-1,-x,z
#6 -x+y-2,-x-1,z+1  #7 -y-1,x-y+1,z+1  #8 x,y,z+1  #9 x-y-1,-y-1,z-1  #10 -x+y-1,-x-1,z-1  #11
-x-2,-x+y-1,z  #12 -x-2,-x+y-1,z-1  #13 x,y,z-1  #14 x-y-1,-y-1,z  #15 -x+y-2,-x-1,z  #16
x-y,-y,z  #17 -y-1,x-y,z  #18 -x+y-1,-x-1,z+1  #19 -y-1,x-y,z+1  #20 -y,x-y+1,z  #21 -
x+y-2,-x-1,z-1  #22 -y-1,x-y+1,z-1
```

Table S5. Anisotropic displacement parameters ($\text{\AA}^2 \times 10^3$) for $\text{LiBa}_3\text{Bi}_6(\text{SeO}_3)_7\text{F}_{11}$. The anisotropic displacement factor exponent takes the form: $-2\pi^2 [h^2 a^{*2} U_{11} + \dots + 2hka^* b^* U_{12}]$

	U11	U22	U33	U23	U13	U12
Bi(1)	9(1)	8(1)	13(1)	0	-1(1)	4(1)
Bi(2)	20(1)	8(1)	13(1)	0	3(1)	4(1)
Ba(1)	9(1)	12(1)	14(1)	3(1)	0	4(1)
Se(1)	7(1)	8(1)	13(1)	0	0(1)	4(1)
Se(2)	8(1)	8(1)	14(1)	0	0	4(1)
Se(3)	7(1)	7(1)	13(1)	0	0	3(1)
F(1)	13(5)	10(3)	24(5)	-3(3)	0	6(2)
F(2)	19(4)	19(4)	7(4)	0	-6(3)	10(2)
O(2)	7(4)	10(4)	19(4)	6(3)	6(3)	0(3)
F(3)	36(7)	36(7)	34(11)	0	0	18(4)
O(3)	7(4)	13(4)	26(5)	2(4)	0(3)	2(3)
O(4)	18(5)	21(7)	13(5)	0	6(4)	11(3)
F(4)	12(3)	9(5)	21(5)	0	6(3)	5(2)
F(5)	25(6)	25(6)	31(10)	0	0	13(3)

Table S6. Atomic coordinates ($\times 10^4$), equivalent isotropic displacement parameters ($\text{\AA}^2 \times 10^3$) for $\text{Ba}_3\text{Bi}_{6.5}(\text{SeO}_3)_7\text{F}_{10.5}\text{O}_{0.5}$.

	x	y	z	U(eq)	Occupy
Bi(1)	2457(1)	10000	2729(1)	14(1)	/
Bi(2)	2613(2)	10000	-1588(2)	28(1)	/
Ba(1)	5871(2)	10000	5520(3)	16(1)	/
Se(1)	3333	6667	2677(5)	16(1)	/
Se(2)	3333	6667	-2115(5)	11(1)	/
Se(3)	6170(4)	10000	467(4)	12(1)	/
F(1)	0	10000	2150(50)	39(12)	/
O(2)	2888(19)	7962(19)	-2984(17)	13(4)	/
O(1)	8096(19)	11630(20)	321(19)	20(4)	/
O(3)	5320(30)	10000	-1040(30)	28(7)	/
O(4)	3390(20)	8260(20)	3530(20)	29(5)	/
F(2)	0	7480(20)	3250(30)	30(6)	/
O(5)	0	10000	-600(60)	53(16)	co-
F(5)	0	10000	-600(60)	53(16)	co-
Bi(3)	0	10420(20)	-4100(20)	109(11)	disorde

					r
F(3)	0	8300(30)	-2860(30)	50(8)	/
F(4)	2360(20)	10000	4910(20)	41(7)	/

U_{eq} is defined as one third of the trace of the orthogonalized U_{ij} tensor.

Table S7. Selected bond lengths [Å] and angles [deg] for $\text{Ba}_3\text{Bi}_{6.5}(\text{SeO}_3)_7\text{F}_{10.5}\text{O}_{0.5}$.

Bi(1)-F(4)	2.09(2)	O(1)#4-Bi(2)-O(1)#5	81.1(8)
Bi(1)-O(4)#1	2.358(18)	O(1)#4-Bi(2)-O(2)#1	88.6(5)
Bi(1)-O(4)	2.358(18)	O(1)#5-Bi(2)-O(2)#1	149.1(6)
Bi(1)-F(1)	2.394(12)	O(1)#4-Bi(2)-O(2)	149.1(6)
Bi(1)-F(2)#2	2.411(12)	O(1)#5-Bi(2)-O(2)	88.6(5)
Bi(1)-F(2)	2.411(12)	O(2)#1-Bi(2)-O(2)	85.4(7)
Bi(2)-O(1)#4	2.404(17)	O(1)#4-Bi(2)-F(3)#2	89.8(7)
Bi(2)-O(1)#5	2.404(17)	O(1)#5-Bi(2)-F(3)#2	136.6(6)
Bi(2)-O(2)#1	2.467(16)	O(2)#1-Bi(2)-F(3)#2	71.9(6)
Bi(2)-O(2)	2.467(16)	O(2)-Bi(2)-F(3)#2	116.7(7)
Bi(2)-F(3)#2	2.494(13)	O(1)#4-Bi(2)-F(3)	136.6(6)
Bi(2)-F(3)	2.494(13)	O(1)#5-Bi(2)-F(3)	89.8(7)
Bi(2)-O(3)	2.62(3)	O(2)#1-Bi(2)-F(3)	116.7(7)
Bi(2)-O(5)	2.65(2)	O(2)-Bi(2)-F(3)	71.9(6)
Ba(1)-F(2)#7	2.65(2)	F(3)#2-Bi(2)-F(3)	68.3(12)
Ba(1)-F(3)#8	2.77(2)	O(1)#4-Bi(2)-O(3)	81.9(6)
Ba(1)-O(4)#1	2.827(18)	O(1)#5-Bi(2)-O(3)	81.9(6)
Ba(1)-O(4)	2.827(19)	O(2)#1-Bi(2)-O(3)	67.8(5)
Ba(1)-O(2)#9	2.836(16)	O(2)-Bi(2)-O(3)	67.8(5)
Ba(1)-O(2)#8	2.836(16)	F(3)#2-Bi(2)-O(3)	138.9(6)
Ba(1)-O(2)#10	2.884(16)	F(3)-Bi(2)-O(3)	138.9(6)
Ba(1)-O(2)#11	2.884(16)	O(1)#4-Bi(2)-O(5)	73.6(10)
Se(1)-O(4)	1.693(18)	O(1)#5-Bi(2)-O(5)	73.6(10)
Se(1)-O(4)#14	1.693(18)	O(2)#1-Bi(2)-O(5)	131.1(6)
Se(1)-O(4)#7	1.693(18)	O(2)-Bi(2)-O(5)	131.1(6)
Se(2)-O(2)	1.702(15)	F(3)#2-Bi(2)-O(5)	63.2(11)
Se(2)-O(2)#14	1.702(15)	F(3)-Bi(2)-O(5)	63.2(11)
Se(2)-O(2)#7	1.702(15)	O(3)-Bi(2)-O(5)	147.5(14)
Se(3)-O(3)	1.65(3)	O(4)-Se(1)-O(4)#14	98.6(9)
Se(3)-O(1)#1	1.709(16)	O(4)-Se(1)-O(4)#7	98.6(9)
Se(3)-O(1)	1.709(16)	O(4)#14-Se(1)-O(4)#7	98.6(9)

Bi(3)-F(3)#2	1.88(3)	O(2)-Se(2)-O(2)#14	98.2(7)
Bi(3)-F(3)#6	1.88(3)	O(2)-Se(2)-O(2)#7	98.2(7)
Bi(3)-F(4)#15	2.07(3)	O(2)#14-Se(2)-O(2)#7	98.2(7)
Bi(3)-F(3)	2.34(3)	O(3)-Se(3)-O(1)#1	103.4(8)
Bi(3)-F(4)#16	2.63(2)	O(3)-Se(3)-O(1)	103.4(8)
Bi(3)-F(4)#17	2.63(2)	O(1)#1-Se(3)-O(1)	103.1(12)
F(4)-Bi(1)-O(4)#1	73.0(7)	F(3)#2-Bi(3)-F(3)#6	96.0(15)
F(4)-Bi(1)-O(4)	73.0(7)	F(3)#2-Bi(3)-F(4)#15	95.4(11)
O(4)#1-Bi(1)-O(4)	74.7(9)	F(3)#6-Bi(3)-F(4)#15	95.4(11)
F(4)-Bi(1)-F(1)	100.7(14)	F(3)#2-Bi(3)-F(3)	82.3(12)
O(4)#1-Bi(1)-F(1)	141.3(6)	F(3)#6-Bi(3)-F(3)	82.3(12)
O(4)-Bi(1)-F(1)	141.3(6)	F(4)#15-Bi(3)-F(3)	176.5(13)
F(4)-Bi(1)-F(2)#2	76.7(7)	F(3)#2-Bi(3)-F(4)#16	154.0(14)
O(4)#1-Bi(1)-F(2)#2	75.8(6)	F(3)#6-Bi(3)-F(4)#16	78.8(6)
O(4)-Bi(1)-F(2)#2	142.6(7)	F(4)#15-Bi(3)-F(4)#16	110.4(10)
F(1)-Bi(1)-F(2)#2	65.8(6)	F(3)-Bi(3)-F(4)#16	71.8(7)
F(4)-Bi(1)-F(2)	76.7(7)	F(3)#2-Bi(3)-F(4)#17	78.8(6)
O(4)#1-Bi(1)-F(2)	142.6(7)	F(3)#6-Bi(3)-F(4)#17	154.0(14)
O(4)-Bi(1)-F(2)	75.8(6)	F(4)#15-Bi(3)-F(4)#17	110.4(10)
F(1)-Bi(1)-F(2)	65.8(6)	F(3)-Bi(3)-F(4)#17	71.8(7)
F(2)#2-Bi(1)-F(2)	118.0(9)	F(4)#16-Bi(3)-F(4)#17	94.7(8)

Symmetry transformations used to generate equivalent atoms:

#1 x-y+1,-y+2,z #2 -y+1,x-y+2,z #3 -x+y-1,-x+1,z+1 #4 -x+y,-x+2,z #5 y-1,x,z
#6 -x+y-1,-x+1,z #7 -x+y,-x+1,z #8 -x+y,-x+1,z+1 #9 y,x+1,z+1 #10 x-y+1,-y+2,z+1
#11 x,y,z+1 #12 x+1,y,z+1 #13 -y+2,x-y+2,z+1 #14 -y+1,x-y+1,z #15 -y+1,x-y+2,z-1 #16
-x+y-1,-x+1,z-1 #17 x,y,z-1 #18 -y+1,x-y+1,z-1 #19 -x+y,-x+1,z-1 #20 -y+2,x-y+2,z #21
-y+1,x-y+2,z+1

Table S8. Anisotropic displacement parameters ($\text{\AA}^2 \times 10^3$) for $\text{Ba}_3\text{Bi}_{6.5}(\text{SeO}_3)_7\text{F}_{10.5}\text{O}_{0.5}$. The anisotropic displacement factor exponent takes the form: $-2\pi^2 [h^2 a^{*2} U_{11} + \dots + 2hka^* b^* U_{12}]$

	U11	U22	U33	U23	U13	U12
Bi(1)	14(1)	10(1)	17(1)	0	2(1)	5(1)
Bi(2)	46(1)	11(1)	16(1)	0	-1(1)	6(1)
Ba(1)	19(1)	10(1)	16(1)	0	-3(1)	5(1)
Se(1)	11(1)	11(1)	26(3)	0	0	6(1)
Se(2)	9(1)	9(1)	14(2)	0	0	4(1)
Se(3)	9(1)	10(2)	17(2)	0	2(1)	5(1)
F(1)	10(12)	10(12)	100(40)	0	0	5(6)

O(2)	17(8)	19(8)	10(8)	7(7)	1(7)	14(7)
O(1)	12(9)	17(10)	25(11)	-1(8)	4(8)	4(8)
O(3)	24(11)	39(19)	26(16)	0	-3(11)	20(9)
O(4)	27(9)	20(9)	49(10)	-6(8)	-15(8)	19(8)
F(2)	5(12)	28(10)	47(17)	-1(11)	0	3(6)
O(5)	27(18)	27(18)	110(50)	0	0	14(9)
F(5)	27(18)	27(18)	110(50)	0	0	14(9)
Bi(3)	22(7)	110(20)	160(15)	-93(15)	0	11(3)
F(3)	65(19)	45(12)	46(18)	-21(12)	0	32(10)
F(4)	40(12)	48(16)	38(16)	0	18(10)	24(8)

Table S9. The calculated dipole moments of the Bi-O(F) polyhedra and the SeO₃ units for LiBa₃Bi₆(SeO₃)₇F₁₁ and Ba₃Bi_{6.5}(SeO₃)₇F_{10.5}O_{0.5} (D = Debyes).

Compound	Species	Dipole moment (D)			
		Total	x(a)-component	y(b)-component	z(c)-component
LiBa ₃ Bi ₆ (SeO ₃) ₇ F ₁₁	Se(1)O3	7.081	4.024	0	5.827
	Se(2)O3	9.929	0	0	-9.929
	Se(3)O3	9.230	0	0	9.230
	Σ[SeO ₃]	6.518	4.024	0	5.128
	Bi(1)O6F2	-1.570	0.775	0	1.366
	Bi(2)O5F2	-9.275	-4.043	0	8.348
	Σ[BiOxFy]	10.249	-3.268	0	9.714
	Unit cell	14.861	0.756	0	14.842
Ba ₃ Bi _{6.5} (SeO ₃) ₇ F _{10.5} O _{0.5}	Se(1)O3	10.567	0	0	10.567
	Se(2)O3	10.511	0	0	-10.511
	Se(3)O3	8.193	4.505	0	-6.843
	Σ[SeO ₃]	8.146	4.505	0	-6.787
	Bi(1)O4F4	-1.906	0.348	0	-1.874
	Bi(2)O6F2	-7.938	5.193	0	-6.004
	Σ[BiOxFy]	9.631	5.541	0	-7.878
	Unit cell	17.776	10.046	0	-14.665

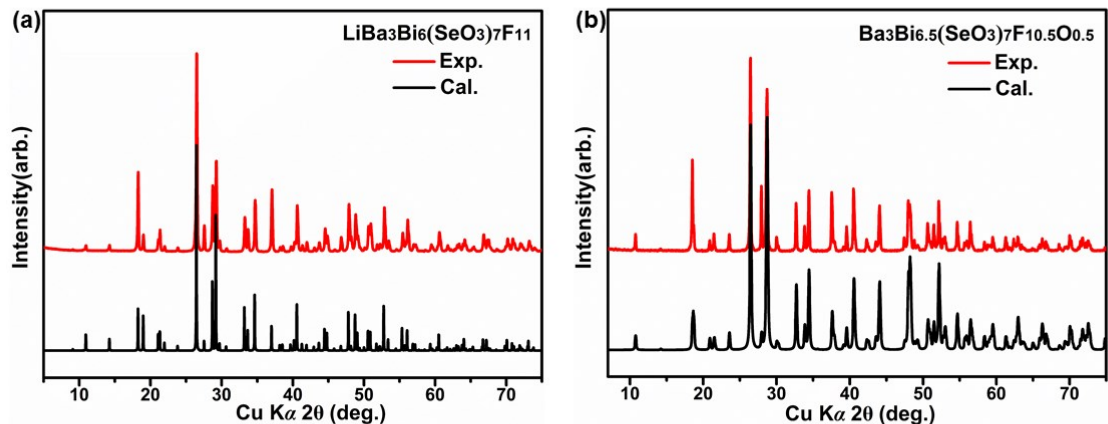


Figure S1. Experimental and calculated powder X-ray diffraction patterns of $\text{LiBa}_3\text{Bi}_6(\text{SeO}_3)_7\text{F}_{11}$ (a) (and $\text{Ba}_3\text{Bi}_{6.5}(\text{SeO}_3)_7\text{F}_{10.5}\text{O}_{0.5}$ (b). The red curve is the experimental one, the black curve is the calculated one.

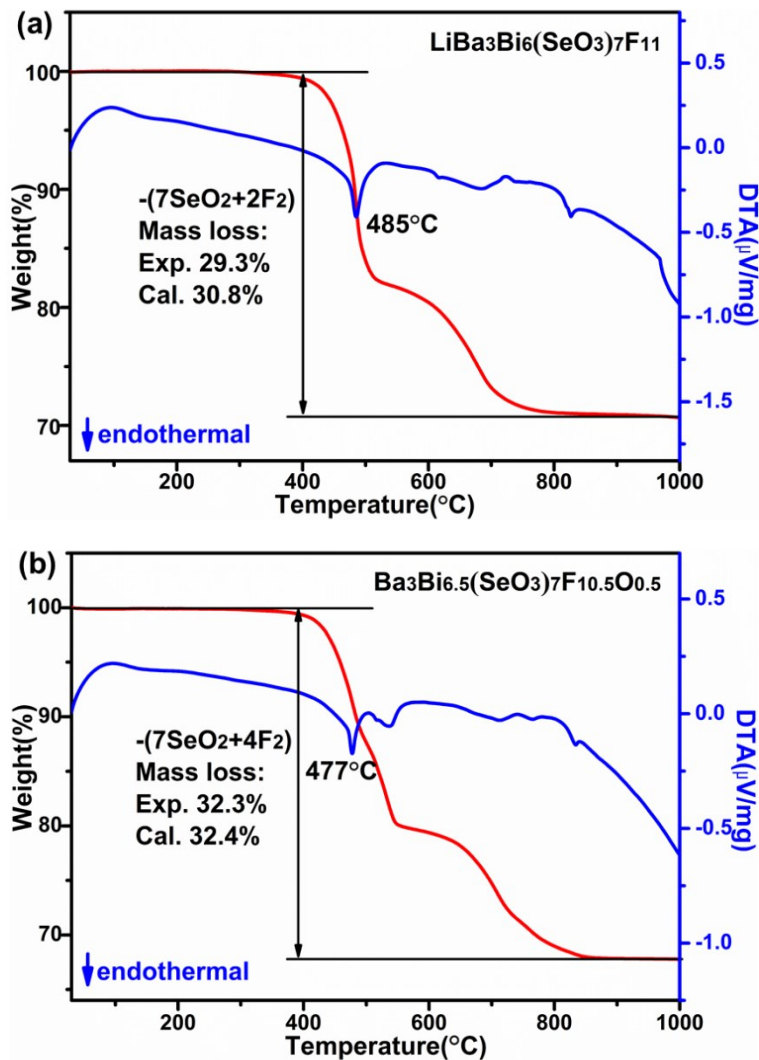


Figure S2. TG and DTA curves of $\text{LiBa}_3\text{Bi}_6(\text{SeO}_3)_7\text{F}_{11}$ (a) and $\text{Ba}_3\text{Bi}_{6.5}(\text{SeO}_3)_7\text{F}_{10.5}\text{O}_{0.5}$ (b).

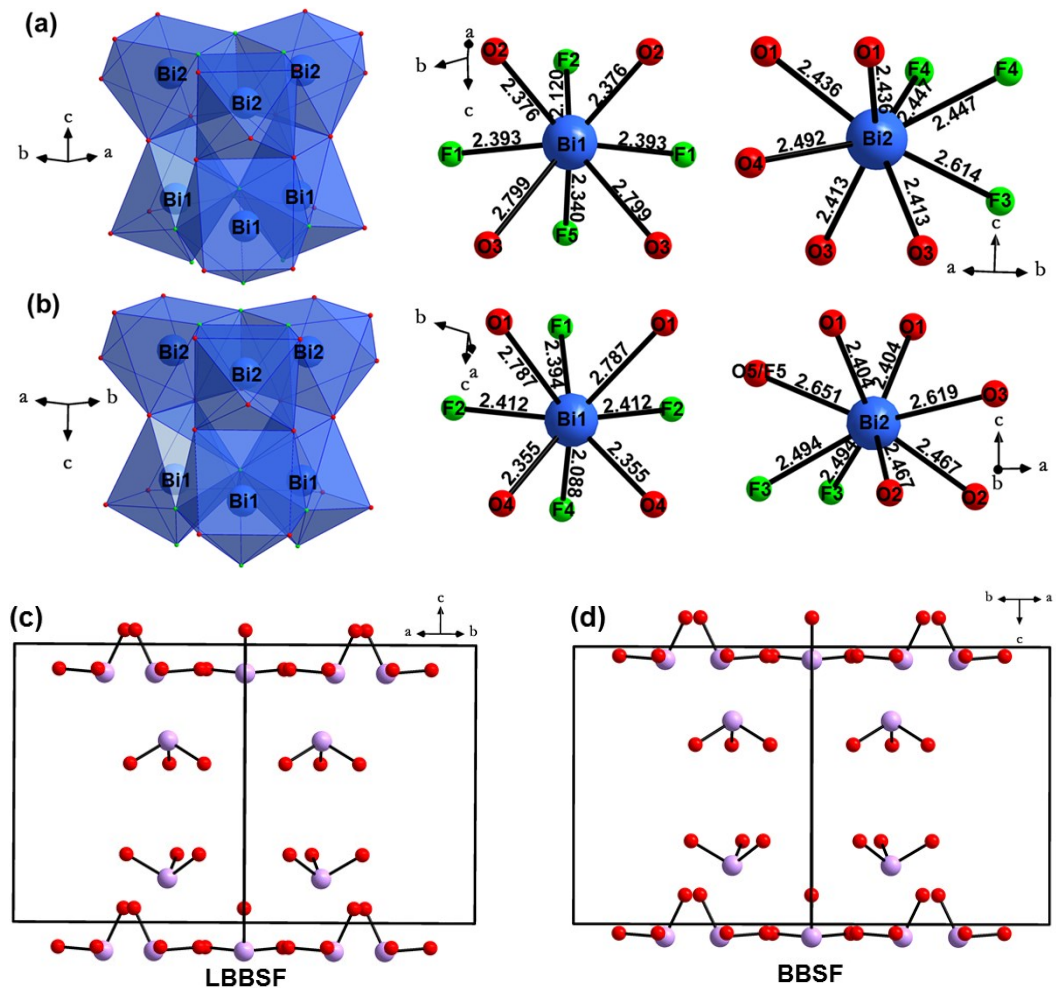


Figure S3. The coordination of Bi atoms of multimers in (a) **LBSF** and (b) **BBSF**, the alignment of [SeO₃] groups in (c) **LBSF** and (d) **BBSF**.

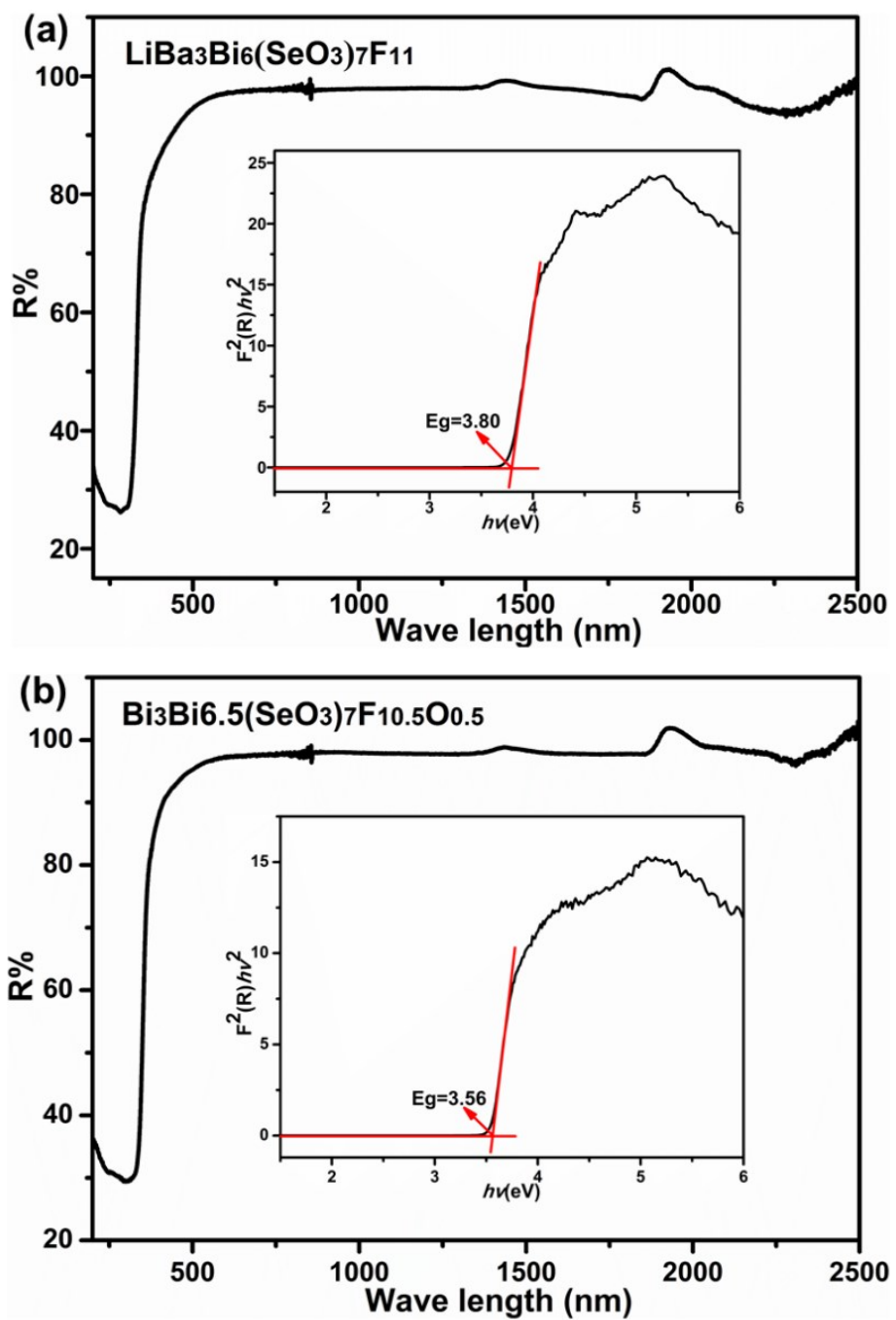


Figure S4. UV-Vis-NIR diffuse reflectance spectra of **LBSF** (a) and **BBSF** (b).

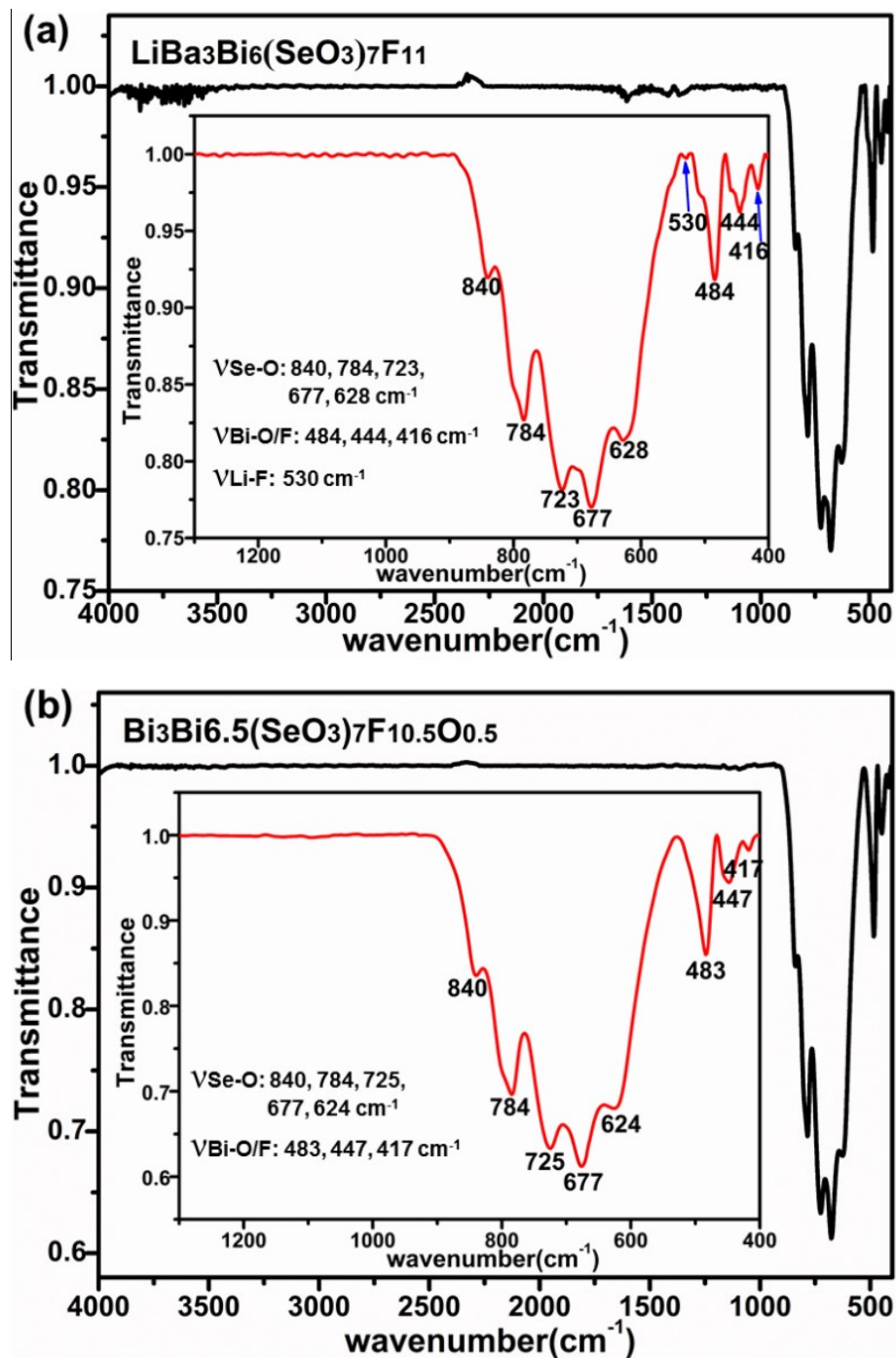


Figure S5. IR transmittance spectra of **LBSF** (a) and **BBSF** (b).

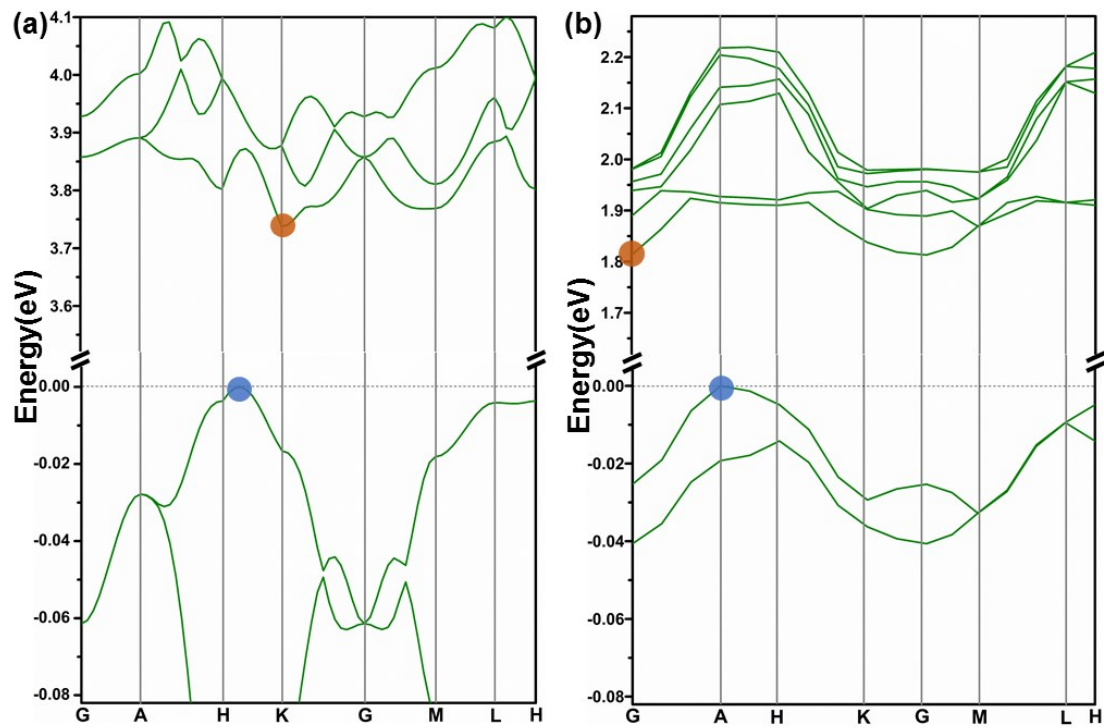


Figure S6. The calculated band structures of **LBBSF** (a) and **BBSF** (b). The drab rounds are at the bottom of conductive band, and the blue rounds suit at the top of valent band.

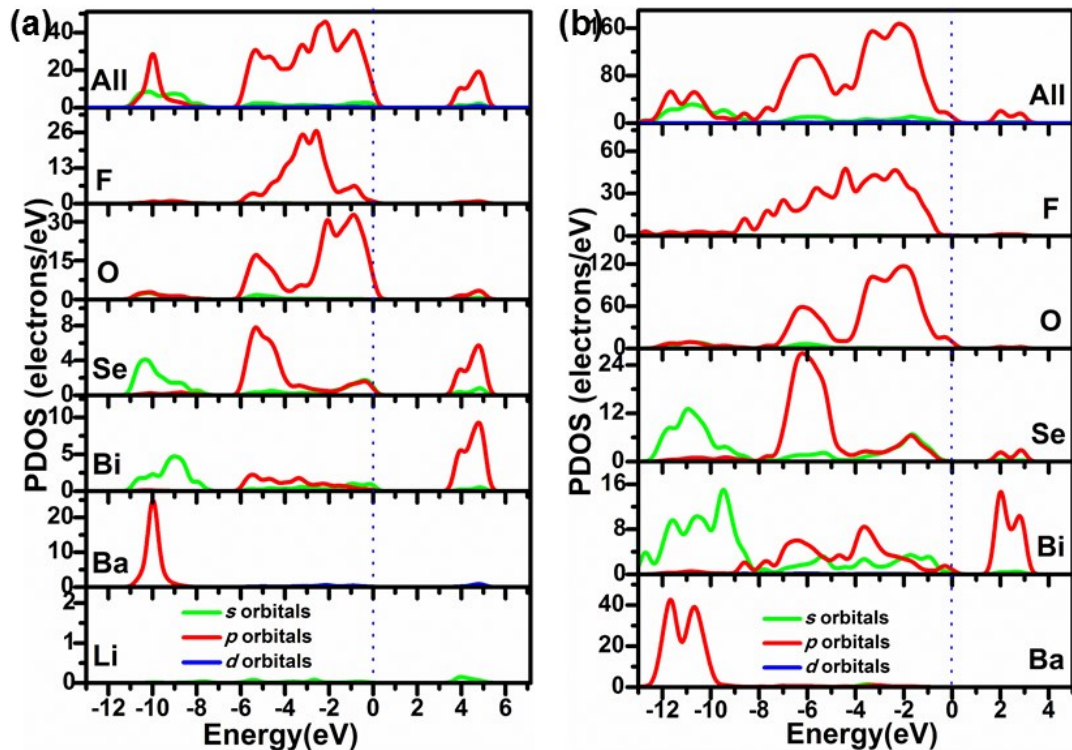


Figure S7. The scissor-added partial density of states (PDOS) for **LBBSF** (a) and **BBSF** (b).

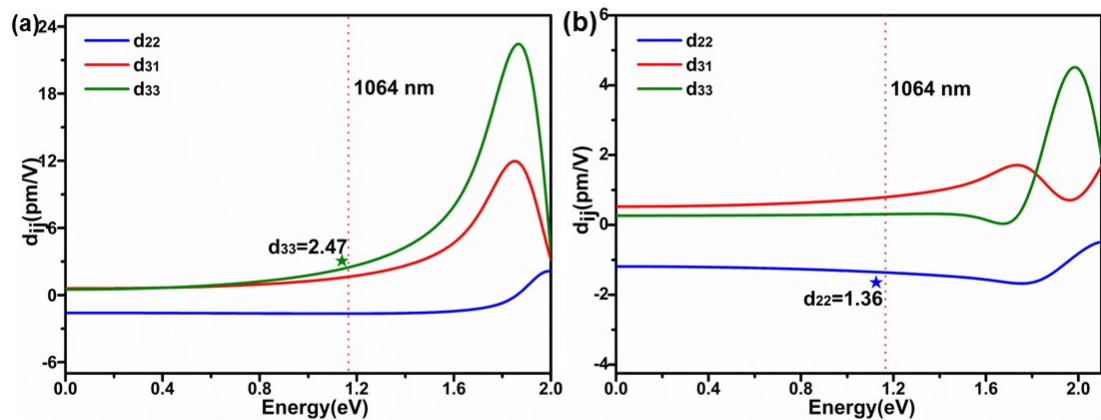


Figure S8. Calculated frequency-dependent SHG coefficients of **LBBSF** (a) and **BBSF** (b).

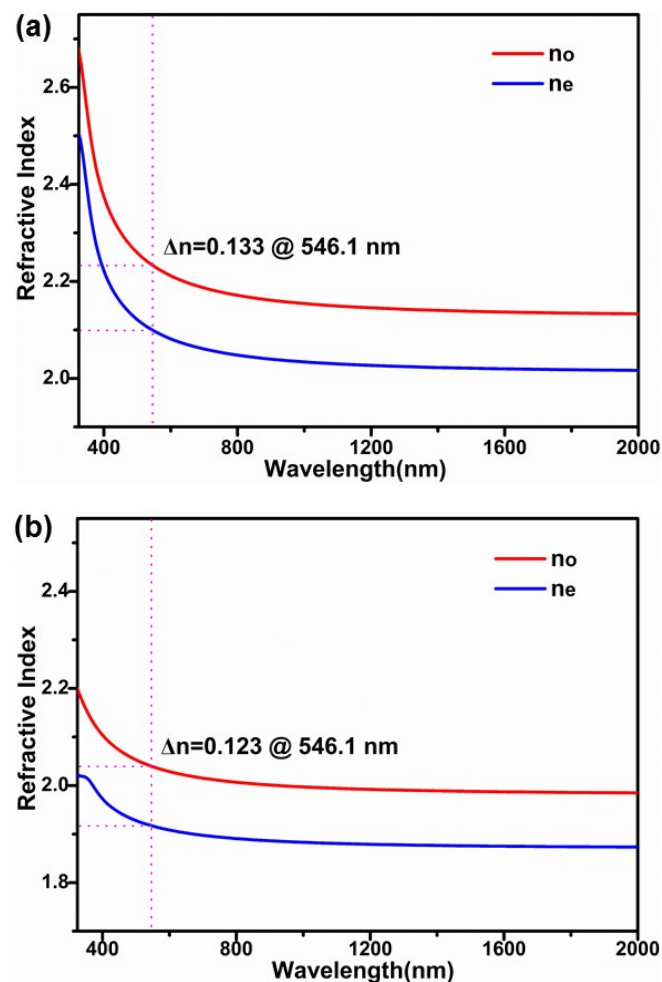


Figure S9. Calculated refractive indices and birefringence of **LBBSF** (a) and **BBSF** (b).

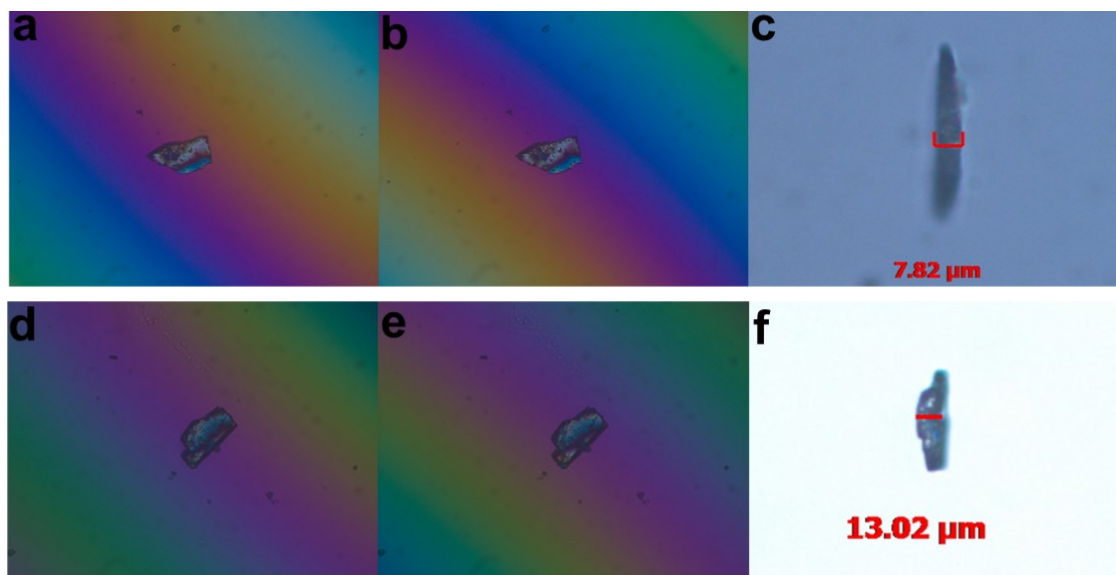


Figure S10. Photographs of **LBBSF** (a-c) and **BBSF** (d-f) for measurements of birefringence.

Reference

1. G. M. Sheldrick, *Acta Crystallogr.*, 2008, **64**, 112.
2. A. L. Spek, *J. Appl. Crystallogr.*, 2003, **36**, 7–13.
3. P. M. Kubelka, F., *Z. Tech. Phys.*, 1931, **12**.
4. J. Tauc, *Mater. Res. Bull.*, 1970, **5**, 721-729.
5. A. Cortes, H. Gomez, R. E. Marotti, G. Riveros and E. A. Dalchiele, *Sol. Energy Mater. Sol. Cells*, 2004, **82**, 21-34.
6. L. L. Cao, G. Peng, W. B. Liao, T. Yan, X. F. Long and N. Ye, *Cryst. Eng. Comm.*, 2020, **22**, 1956-1961.
7. S. K. Kurtz and T. T. Perry, *J. Appl. Phys.*, 1968, **39**, 3798-3813.
8. M. C. Payne, M. P. Teter, D. C. Allan, T. A. Arias and J. D. Joannopoulos, *Rev. Mod. Phys.*, 1992, **64**, 1045-1097.
9. S. J. Clark, M. D. Segall, C. J. Pickard, P. J. Hasnip, M. J. Probert, K. Refson and M. C. Payne, *Z. Kristallogr.*, 2005, **220**, 567-570.
10. A. M. Rappe, K. M. Rabe, E. Kaxiras and J. D. Joannopoulos, *Phys. Rev. B*, 1990, **41**, 1227-1230.
11. H. J. Monkhorst and J. D. Pack, *Phys. Rev. B*, 1976, **13**, 5188-5192.
12. R. W. Godby, M. Schluter and L. J. Sham, *Phys. Rev. B*, 1988, **37**, 10159-10175.
13. K. S. Virk and J. E. Sipe, *Phys. Rev. B*, 2007, **76**, 035213.
14. M. H. Lee, C. H. Yang and J. H. Jan, *Phys. Rev. B*, 2004, **70**, 235110.